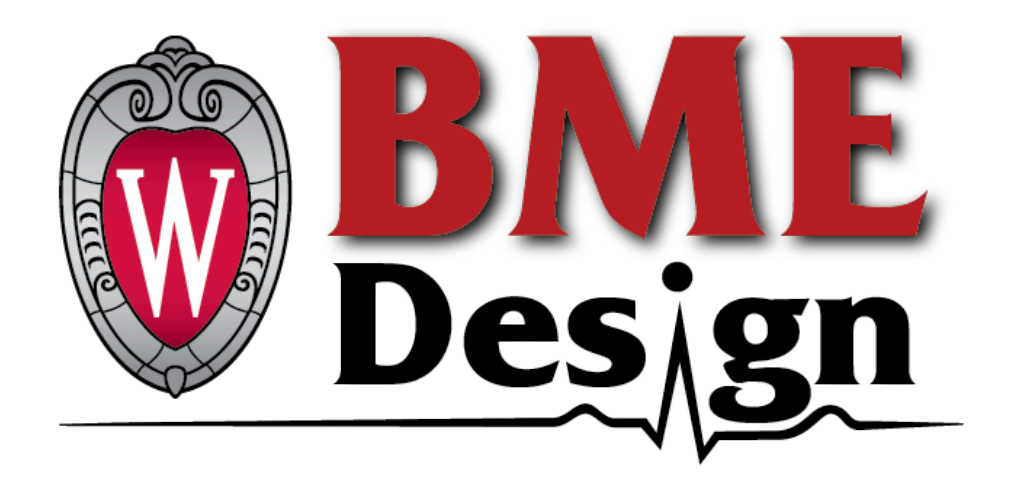
# Intracranial EEG Phantom for Brain Stimulation Studies Preliminary Report



BME 400 13 October 2025

Clients: Dr. Raheel Ahmed, Dr. Arun Manattu
UW School of Medicine and Public Health
Neurosurgery

Advisor: Dr. Paul Campagnola
University of Wisconsin–Madison
Department Chair of Biomedical Engineering

# Section 303

Avery Schuda (Team Leader) - aschuda@wisc.edu
Lilly Mackenzie (Communicator) - lfmackenzie@wisc.edu
Orla Ryan (BWIG)- orryan@wisc.edu
Helene Schroeder (BSAC) - hschroeder4@wisc.edu
Corissa Hutmaker (BPAG) - hutmaker@wisc.edu

# **Abstract**

Epilepsy is a prevalent neurological condition marked by the occurrence of repeated, uncontrollable seizures. This disorder can present in individuals of all ages, but commonly manifests in children. Suitable treatment is therefore of high priority, especially in these pediatric patients, to improve quality of life. One main treatment method is that of surgical intervention, in which neurosurgeons identify and disconnect cranial regions involved in seizure generation. Prior to these operations, brain mapping techniques such as intracranial electroencephalography (iEEG) and transcranial magnetic stimulation (TMS) are utilized to delineate brain connectivity: using these methods in tandem would be ideal for providing the quickest, most accurate care possible. As such, a brain phantom model composed of a hydrogel solution and encased in clear resin will be developed that can be used to simulate the main effects of TMS on iEEG electrodes. By considering criteria such as substance reactivity, mechanical properties, shelf life, and preparation techniques, the preliminary materials chosen are an agar-based hydrogel brain model surrounded by FormLabs BioMed Clear resin. Upon fabrication of an initial agar solution, several rounds of preliminary testing will be performed to ascertain the ideal solution composition. Subsequently, testing methods for measurements of temperature changes, electrical conductivity, and electrode displacement will be refined and followed to overall simulate accurate pediatric brain tissue behavior.

# **Table of Contents**

Abstract	1
<b>Table of Contents</b>	2
I. Introduction	3
Motivation	3
Existing Devices	3
Problem Statement	4
II. Background	4
Client Information	5
Design Specifications	5
III. Preliminary Designs	5
Hydrogel Material	5
Skull Material	6
IV. Preliminary Design Evaluation	7
Design Matrices and Summary	7
Proposed Final Design	11
V. Fabrication	12
Materials	12
Methods	13
Final Prototype	13
VI. Testing	13
VII. Discussion	14
VIII. Conclusions	15
References	16
Appendix	17
A. Product Design Specifications (PDS)	17
B. Materials and Expenses	23
C. Minitab for Initial Agar and Saline Ratios	24
D. Use of Rheometer with Hydrogel Testing Protocol	24
E. Hydrogel Thermal Conductivity Testing Protocol	25
F. Electrode Displacement Testing Protocol	26
G. Electrode Heating Testing Protocol	26
H. Electrode Current Generation Testing Protocol	26

# I. Introduction

#### Motivation

There are a range of neurological disorders, each capable of causing a profound impact on an individual's life. Epilepsy, as the fourth most common neurological disease, is characterized by the regular appearance of uncontrollable seizures. The disorder can be highly detrimental to one's ability to thrive, and is associated with a higher risk of depression, accidents, and death. People of all ages can be affected by this disease, and it often manifests before the age of one year [1]. Despite this broad demographic, there is a significant lack of research and clinical explorations in pediatric patients, possibly due to the complicated ethical challenges surrounding the participation of children in human studies [2].

The obstacles that impede research studies utilizing pediatric participants may result in a gap of treatment knowledge. As such, constructing study tools that can spur on discoveries targeted towards this younger population is of great importance. An area of exploration tied to epilepsy is that of various treatment methods. Aside from the use of medication, surgical management is an oft-investigated treatment tool in the control of epileptic seizures. Prior to surgical intervention, which may involve procedures such as temporal lobectomies, or removal of certain portions of the brain, a variety of brain mapping techniques such as intracranial electroencephalography (iEEG) and transcranial magnetic stimulation (TMS) are utilized to provide a guide for neurosurgeons. These techniques, involving implanted electrodes and applied magnetic simulation, respectively, have been tested on phantom models before being applied to human subjects to certify their level of risk and effectiveness [3].

# **Existing Devices**

There exist brain phantoms that have been used in research settings, but none achieve the specifications as required by this project. Researchers at the University of Iowa created a gel-based brain phantom to prove that TMS and iEEG can be safely used in tandem, specifically in adult patients. The brain of this phantom was made of poly(acrylic acid) (PAA) saline gel, and the skull was made of poly(methyl methacrylate) (PMMA). The researchers on this project determined if combined use was safe by analyzing the change in temperature of the electrodes, displacement of the electrodes, and introduction of secondary electric currents. The results of this study showed that the combined use of TMS and iEEG are safe for adults, which is similar to the goal of this project, except that this project focuses on pediatric patients [3]. There are different physiological and electrical properties between the adult and pediatric brain, as well as different safety considerations to be taken into account. Because of these differences, The University of Iowa's gel phantom cannot be used to determine if TMS and iEEG are safe in pediatric patients. Pediatric brain phantoms do exist, but none meet the scope of this project. For example, there is a 3D-printed pediatric head phantom that accurately depicts the size and shape of a pediatric brain, but was fabricated to create an optimized protocol for pediatric computed tomography (CT)

imaging. The brain of this phantom was made with epoxy resin, and the skull was made with plaster and resin [3]. As mentioned previously, the size and shape of the 3D-printed phantom matches this project, but there are no other similarities in their functionality.

#### **Problem Statement**

The goal of this project, therefore, is to develop a pediatric brain phantom model that can be used to simulate the main effects of TMS on iEEG electrodes – induced currents, temperatures, and changes in position – in order to verify that these brain mapping techniques can be used in tandem.

# II. Background

As previously described, epilepsy is a complex neurological condition in which recurrent unprovoked seizures occur. These seizures are caused by short, excessive discharge of electrical activity in the brain: the abnormal propagation of electrical impulses can be caused by insufficient inhibition, excessive excitation, or a combination of both factors within the brain's neuronal network [1]. Various lobes within the cerebral cortex can be involved in seizure generation, each associated with differing symptoms or manifestations. There are several antiepileptic pharmacological treatments utilized in treating epilepsy, including both narrow-spectrum drugs that work for specific seizure types and broad-spectrum drugs that have some efficacy for a wider range of seizures. About 30% of patients have drug resistant epilepsy, however; in this case, another treatment option considered is that of surgical intervention. The mortality rate in children affected by epilepsy is 5-10 times higher than the rest of the population, so properly treating and controlling these unprovoked seizures is paramount [4].

The surgical approaches taken when pursuing epilepsy treatment can vary widely, depending on patient-specific pathology. As a whole, the techniques used prioritize minimal invasive procedures that still target epileptogenic zones. These zones are classified as the regions of the brain that are capable of generating seizures; upon removal or disconnection of these areas, seizure freedom can potentially be obtained [5]. Prior to undergoing operation, brain mapping techniques can generate spatial representations of the patient's brain to map out which regions are presenting abnormal behavior. One such method, iEEG, is routinely used in surgical planning and utilizes electrode systems that are either connected across the surface of or implanted into the brain. This method provides high spatiotemporal resolution and is especially advantageous for epileptogenic foci localization [6]. TMS, another technique, assesses brain circuit excitability through electromagnetic induction, inducing currents to produce action potentials and painlessly activate brain networks [7]. TMS is renowned for its noninvasive nature, as well as its capability to illustrate brain connectivity. As a result, both techniques may provide complementary information for mapping out critical brain regions that should be avoided during surgery. However, there are several safety concerns around the use of TMS in patients with iEEG: that of secondary electrical currents, heating of the implanted electrodes, and

electrode array displacement, all of which would have severe consequences for the affected individuals [3]. Additionally, the impact of these techniques has not been previously studied on children with epilepsy, but instead on adult patients; dissimilar physiology and comparative higher resting motor thresholds might require higher levels of stimulation, both of which indicate the need for adjusted treatment [8].

#### **Client Information**

The client for this project is Dr. Ahmed, a pediatric neurosurgeon at the American Family Children's Hospital (AFCH) who has a focus in pediatric epilepsy. The alternate contact for this project is Dr. Manattu, a scientist at the Waisman Center's Pediatric Neuromodulation Laboratory (PNL).

# **Design Specifications**

The phantom must accurately represent the physiology of an average pediatric brain and skull, with a skull circumference of 50-54 cm and overall volume of 1,300 cm $^3$  [] []. The material chosen for the brain must have a similar electrical conductivity as brain tissue, 0.2-0.5 S/m []. After TMS testing with the phantom is complete, there must be a less than 1 °C temperature change in the electrodes. There must also be a less than 30  $\mu$ C/cm $^2$  change in charge density of the electrodes and minimal displacement of the electrodes. See Appendix A for full design specifications.

# **III.** Preliminary Designs

# **Hydrogel Material**

## **Gelatin**

Gelatin is a natural protein that is derived from the hydrolysis of collagen. Gelatin is widely used as a hydrogel due to its biodegradability, accessibility, and low cost. Its gelation is thermo-reversible at approximately 20-25 °C [9]. Gelatin's preparation includes polymerization, crosslinking, and hydrolysis. Adjusting the concentration or crosslinking of gelatin during its preparation can change the properties of the hydrogel like porosity, stiffness, and degradation rate [10].

## Poly(acrylic acid) (PAA)

PAA is a synthetic polymer derived from the polymerization of acrylic acid. Despite being synthetic, PAA still shares many of the positive characteristics of natural hydrogels, such as being biodegradable, nontoxic, and biocompatible. As a synthetic material, PAA can be easily tuned to increase its mechanical properties via crosslinking or copolymerization [11].

## <u>Agar</u>

Agar is a polysaccharide derived from the cell walls of seaweed. Agar is widely used in biomedical applications due to its biocompatibility and strong ability to gel. Agar is composed of a blend of agarose and agarose pectin, in which the agarose component allows for gelling. Gelation is thermoreversible and occurs slightly above body temperature. The mechanical properties of agar are generally considered to be low, but can be tuned by changing the concentration of agar, crosslinking, or incorporating other materials [12].

# <u>Agarose</u>

Agarose is a polysaccharide derived from red algae, or seaweed, and is a purified form of agar. Agarose exhibits good biocompatibility, biodegradability, and thermoreversible gelling which make it able to be widely used in biomedical applications. Chemical or physical modifications allow agarose to be versatile and used in many different environments. The gelation of agarose occurs below or around body temperature and this process is thermoreversible. Agarose on its own is considered to be brittle but enzymatic modifications can improve this property. Processes like crosslinking can be used to tune agarose to the desired mechanical properties [13].

#### **Skull Material**

# Poly(lactic acid) (PLA)

PLA is a thermoplastic polymer that is widely used in engineering and biomedical applications due to its biodegradable, biocompatible, and nontoxic properties. PLA is often derived from renewable materials such as corn starch and sugarcane, and is most commonly used for rapid prototyping via 3D printing due to its wide accessibility and low cost [14]. While PLA has many advantages, it is considered disadvantageous due to its brittleness, low toughness, and slow crystallization rate [15]. The elastic modulus of PLA is 3.5 gigapascals (GPa) and its tensile strength is 50 megapascals (MPa) [16].

# Poly(methyl methacrylate) (PMMA)

PMMA is a thermoplastic polymer widely used in resin 3D printing which has a wide variety of possible molecular weights. Using different molecular weights of PMMA can change properties such as viscosity, elastic modulus, and brittleness. PMMA is considered advantageous due to its transparency and high strength. The elastic modulus of PMMA is between 18 and 31 GPa [17].

# FormLabs BioMed Clear Resin (FBC)

FBC resin is a material commonly used for biomedical applications where there is long-term contact with the skin or mucosal membrane due to its biocompatibility. FBC resin is printed by FormLabs stereolithography (SLA) printers and may have a clear finish. FBC resin is compatible with common sterilization methods, including autoclaving and ethylene oxide

sterilization, which make FBC versatile for many different applications. The elastic modulus of FBC resin is 2.08 GPa and its tensile strength is 52 MPa [18].

# FormLabs Standard Resin (FS)

FS resin is a material that is commonly used for creating parts that require showcasing internal features, like fluidic devices, due to its highly transparent nature. FS resin is printed by a FormLabs SLA printer, capable of a quick printing speed while maintaining accuracy. The tensile strength of FS resin is between 46 and 60 MPa [19].

# IV. Preliminary Design Evaluation

# **Design Matrices and Summary**

**Table 1: Hydrogel Material** 

Design Criteria	Weight	Gel	atin	Poly(a	nerylic id)	Αg	gar	Agarose		
Thermal Conductivity	20	2/5	8	3/5	12	5/5	20	1/5	4	
Preparation	20	2/5	8	4/5	12	5/5 20		4/5	16	
Tunability	20	1/5 5		5/5	20	3/5	12	3/5	12	
Reactivity	15	4/5 12		3/5	9	2/5	6	3/5	9	
Shelf Life	15	1/5	3	4/5	12	3/5	9	3/5	12	
Cost	10	5/5	10	2/5	4	4/5	8	2/5	4	
Total	100	46		6	9	7	5	57		

# Thermal Conductivity

The thermal conductivity criteria analyzes how easily a material conducts heat. A high thermal conductivity value indicates the material is a great conductor and readily passes heat. The brain has a thermal conductivity of 0.536 W/m-K, and the chosen material should be within a similar range [20]. Agar was a close match to the thermal conductivity of the brain, measuring 0.52 W/m-K [21]. PAA and gelatin were slightly less than this at 0.37 and 0.30 W/m-K, respectively [22], [23]. The thermal conductivity of agarose was significantly less than the brain, only offering conductivity of 0.121 W/m-K [24].

# **Preparation**

Preparation is defined as the level of difficulty that is required to prepare the hydrogel, as well as the methods of fabrication possible for each material and their compatibility with this project. Factors like time and amount of materials needed are considered in the difficulty of preparation. The hydrogel that requires the least amount of time and materials will score the highest. An ideal hydrogel will also be able to take on an anthropomorphic brain shape, most easily achieved via a photoactivation fabrication technique [25]. Of the reviewed materials, gelatin is the only that requires chemical modification in order to remain stable at room temperature, despite having a relatively simple preparation without these modifications [9]. The required modifications gelatin the lowest score in this category, while agar's simple gelation and greater stability at room temperature gave it the highest score. Agarose and PAA scored intermediately as they both require other materials and multiple steps to prepare.

# **Tunability**

Tunability refers to the ability to adjust various material properties of the hydrogel via changes in its concentration, crosslinking, and other techniques. Material properties are crucial in determining which gel is most similar to the average pediatric brain, but these can differ significantly based on adjustments made to the gel. The gel that scores the highest will be the gel with the best tunability. In general, synthetic polymers are more easily tunable than natural polymers, as they are more controlled and consistent [26]. Because of this, PAA scored the highest as it is the only synthetic material. Gelatin scored the lowest as it is not tunable on its own and requires chemical modifications to become easily tunable [27]. Agar and agarose scored in the middle, as they can be easily modified by changing their concentrations, but are less precise than PAA due to being natural materials.

## <u>Reactivity</u>

Reactivity refers to the hydrogel toxicity levels, compatibility with the skull polymer, and durability throughout each testing period. The hydrogel should pose no significant harm to the handler when performing safe care with the gel such as wearing gloves and avoiding ingestion. The hydrogel also must not induce a reaction of any sort with the exterior skull mold that will encase the internal brain phantom. Lastly, the material must be able to maintain its structure throughout a single testing period with iEEG and TMS, ensuring little variation in results due to external sources. Agar scored the lowest due to its toxicity when inhaled and in contact with the skin [28]. Additionally, it does not maintain its structure as well as the other gels when needle-like items are inserted into the material [29]. PAA scored in the middle because although it is generally non-toxic, it also does not maintain its structure after having items inserted into it [30], [31]. Agarose earned the same score as PAA because although it can recover from item insertion, it has higher toxicity levels [32], [33]. Gelatin was rated the highest because it is non-toxic and will maintain its structural integrity [34], [35]. None of the materials are expected to react with the cured resin material that will be used for the 3D-printed skull.

# Shelf Life

Shelf life is defined as the gel's degradability rate or time before the gel must be replaced during testing. The hydrogel with the slowest degradability rate and longest amount of time before it needs replacement will score the highest, as this gel is the most efficient to use. The gel that scored the lowest was gelatin due to its thermal instability and quick degradation rate [36]. PAA scored the highest as it is a synthetic polymer that is not subject to enzymatic or hydrolytic degradation [37]. Agar and agarose scored intermediately, with degradation rates of weeks to months [38], [39].

# <u>Cost</u>

The cost criteria is the price of each hydrogel per gram. Gelatin is the least expensive material by far, costing \$0.05 per gram [40]. Agar had the next best price being approximately \$0.39 per gram [41]. Lastly, agarose and PAA were given the same ranking, costing \$1.51 and \$1.74 per gram, respectively [42], [43].

**Table 2: Skull Material** 

Design Criteria	Weight	Poly( acid) (			methyl crylate) MA)	Form BioMe		FormLabs Standard Resin		
Reactivity and Shelf Life	25	3/5	3/5 15		25	4/5	4/5 20		15	
Transparency	20	1/5	4	5/5	20	5/5	20	3/5	12	
Permittivity	20	2/5 8		3/5	12	5/5	20	5/5	20	
Accessibility	15	5/5 15		1/5	3	4/5	12	4/5	12	
Mechanical Properties	10	2/5	4	5/5	10	5/5	10	3/5	6	
Cost	10	5/5	10	1/5	2	3/5	6	4/5	8	
Total	100	56		7	2	8	8	73		

## Reactivity/Shelf Life

Reactivity is defined as the relative likelihood of the skull polymer to react with, including enhance the degradation of, the brain phantom hydrogel. Both FormLabs filaments are described as non-reactive under recommended conditions, and have very high boiling and flash points. Shelf life refers to the polymers rate of degradation, especially when exposed to water.

This is primarily relevant to prevent rapid degradation of both the skull material and the subsequent changes to the properties of the hydrogel material caused by reactions with any dissolved skull materials. PMMA, followed by PLA and FBC display the slowest rate of degradation in water. In this category, however, FBC scored highest due to extensive safety and degradation testing with positive results. It is important to note that the reactivity of each skull polymer will depend on the chosen brain hydrogel material – crosslinking agents such as peroxides should be avoided [18].

## **Transparency**

The transparency category describes the need for optical clarity with regards to the brain phantom itself. One of the main focuses of the client is to measure possible displacement of implanted and surface electrodes during the application of TMS current; in order to capture this potential movement, the user must be able to visualize the phantom itself. In a similar recent study, clarity was essential, as a motion capture camera system was used to measure said displacement. As such, two material options scored the highest in this category: PMMA and FBC resin. Both materials are suitably clear, as PMMA is often touted as a glass substitute and FBC resin is recommended for visibility purposes [18], [44].

## **Permittivity**

Permittivity refers to a material's ability to allow electric field generation across it. In the context of this project, permittivity closest to that of cranial bone is preferred: around 2.76 x 10<sup>2</sup> F/m in the case of cancellous bone, and around 1.53 x 10<sup>2</sup> F/m in the case of cortical bone [45]. This value is crucial for accurate testing values and ensuring patient safety. All four polymers displayed similar lower permittivities when compared to cranial bone. PMMA and PLA reported values of 2.76 and 2.5 F/m, respectively, at maximum while FormLabs resin options displayed comparatively higher permittivity values, in the range of 3-4 F/m [46], [47]. Thus, these two materials were deemed closest to physiological, relative permittivities. It is important to consider these differences between physiological and polymeric permittivity when establishing testing procedures.

## **Accessibility**

PMMA was by far the least accessible, due to the fact that it is not stocked as a material option in the University of Wisconsin-Madison's Grainger Design and Innovation Lab at Wendt Commons (DI Lab), leading to the need to outsource a 3D printing service. Options for this would be to submit prints to a fee for printing service, but these prints have a long lead time and no direct control over the printing process. Another option would be to purchase a spool of PMMA filament, requiring access to a printer not at the DI Lab. In contrast PLA, FBC resin, and FS resin are all available to print in the DI Lab. PLA is the most accessible, as it is available on the greatest number of printers and requires no post-processing once the print is complete. Both FormLabs resins are slightly less accessible due to the fact that there are less available FormLabs

printers, and require DI Lab staff to perform post-processing to cure the final print to the desired finish.

# Mechanical Properties

The mechanical properties of the skull material were deemed necessary to consider as well. Although the skull is not under mechanical duress during TMS testing, meaning that tensile or elastic moduli were of little consequence to the material choice, finding a material with appropriate porosity to provide similar supportive capabilities to the human skull was preferable. Once again, both PMMA and the FBC resin were rated the highest in this category. The mean reported elastic modulus for the human skull is around 8.51 GPa; resin has been found to have an elastic modulus of around 2.8 GPa, while acrylic-based polymers reportedly present elastic moduli around 2.15 GPa. As both of these values are on the same magnitude of relevant human skull properties, both materials received high scores [48] . Porosity was also considered, given the reported porousness of human bone. However, this was not factored as heavily into this rating given the inherent capability of 3D-printed parts to achieve a porous structure using a variety of materials [49] .

## <u>Cost</u>

Cost was defined as the cost to 3D print the materials per gram. PLA was by far the most affordable, at \$0.05 per gram. FS resin is the next most affordable at \$0.24 per gram and FBC resin is priced at \$0.42 per gram [14]. While the direct cost of PMMA is typically around \$0.07 per gram, due to a lack of accessibility, there is an upfront cost associated with using this material. One option is the prints would have to be outsourced to a third party 3D printing service, 3ERP, which quoted \$27 per gram to print in PMMA [50]. Another option is purchasing an entire spool of PMMA filament costing in the range of \$50-\$67 for one kilogram [51].

## **Proposed Final Design**

The proposed final design is a head phantom that accurately mimics the size and shape of a pediatric head. The brain of the phantom will be created using an agar hydrogel that incorporates a sodium chloride (NaCl) solution to increase its electrical conductivity to match that of brain tissue. The skull of the phantom will be 3D printed with FBC resin.

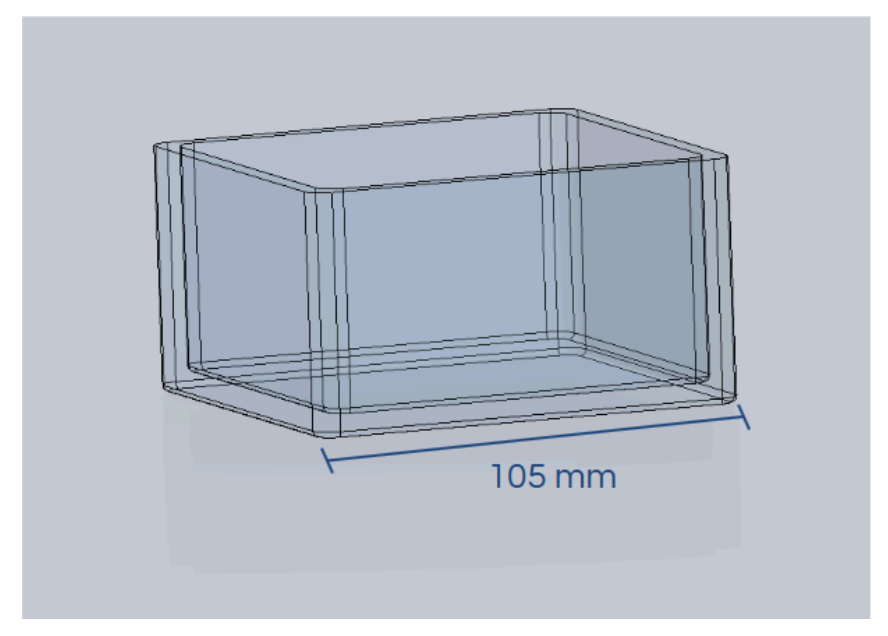


Figure 1: Pediatric sized gel box phantom CAD model.

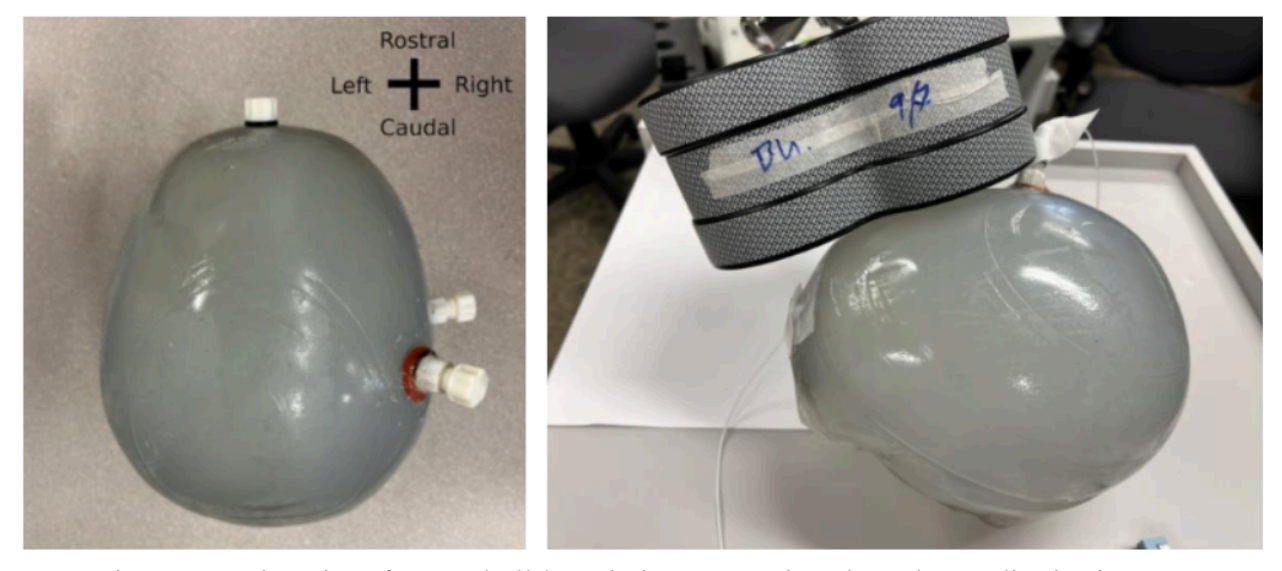


Figure 2: University of Iowa skull-based phantom, to be adapted to pediatric size [3].

# V. Fabrication

# **Materials**

# Skull Base

FBC resin was chosen as the material for the skull base. FBC is an acrylate, urethanedimethacrylate, methacrylate copolymer [52], which has a Young's Modulus of 2.08 GPa [53], consistent to an order of magnitude with the stiffness of cranial bone [48].

Additionally, this material is readily available to 3D print at the DI Lab at the price of \$0.24 per gram [14].

## Brain Tissue Phantom

The project will move forward with an agar-based hydrogel for the brain tissue phantom. Agar is a natural material composed of the polysaccharides agarose and agarose-lectin, which gel via self-assembly into a thermo-reversible state [12]. Agar can also be photopolymerized by the addition of photoactivators, is also highly adjustable with a variety of additives for mechanical and electrical properties [54].

The hydrogel used in this project will be tuned with NaCl for optimal electrical properties, as outlined in Section VI, to match those of native brain tissue. NaCl concentration also has a positive correlation with gel stiffness, which will be accounted for [54], [55]. A powdered form of agar will be used, which is water-soluble and available at ThermoFisher for the price of \$0.26/gram [41].

#### Methods

#### Skull Base

An initial prototype of the brain tissue will be fabricated in a FBC resin rectangular mold, similar to the University of Iowa preliminary phantom [3]. Following preliminary material testing (see Section VI), the final prototype will be fabricated in the size and shape of a pediatric human skull. For further design specifications, see Appendix A.

A human pediatric skull will be modeled in SolidWorks 2025, before printing using a FormLabs Form 4 Stereolithography (SLA) printer. SLA 3D printing involves layer-by-layer deposition of liquid-phase resins, which are UV-cured as they are deposited [56].

## Brain Tissue Phantom

The brain tissue phantom will be fabricated of an agar and NaCl solution, with deionized water composing the excess volume required to achieve required mechanical and electrical properties. Preliminary testing (Section VI) will reveal precise concentrations and volumes of each material required for this phantom.

Briefly, the measured reagents will be mixed in a large beaker, heating the solution up to 90 °C to dissolve the agar powder. The solution will be cooled in a 4 °C freezer until first gelled, before undergoing further polymerization under UV light [54].

# VI. Testing

**Determining Agar and Saline Ratios** 

Minitab software can be used for Design of Experiments (DOE) with the hydrogel as well as the NaCl solution it will be placed in. A full factorial design will be used with 2 factors and 3 levels for a total of 9 treatment combinations. The rounds of testing will be conducted using different ratios of NaCl in water for the saline solution while also using various concentrations of agar hydrogel. The planned saline solutions will be 1%, 3%, and 5% [54], [55]. The planned agar concentrations will be 2%, 4%, and 6% [21], [55]. See Appendix C for the current testing protocol.

# Mechanical Properties of Hydrogel

To determine if the hydrogel properly mimics mechanical properties of brain tissue, mechanical testing must be performed. Part of this testing will be done using a Malvern Kinexus Ultra+ rheometer with parallel plate geometry to analyze the shear and elastic moduli of the hydrogel. The final hydrogel will have a shear modulus of 2.4 to 3.0 kPa and an elastic modulus of 1.08 to 2.49 kPa [57], [58]. The hydrogel thermal conductivity will be within 5% of 0.536 W/m-K and will be tested using the Transient Line Source (TLS) method [20]. See Appendix D and E for planned testing procedures. The amount of agar present will be altered until the hydrogel closely reflects brain tissue material.

# Electrode Displacement

Positioning of the electrodes must be measured before and after application of TMS to ensure minimal displacement is occurring. There should be no measurable movement of electrodes due to the implanted nature of depth electrodes. See Appendix F for the testing procedure.

## Electrode Heating

Temperature of the tissue surrounding implanted electrodes will be taken before and after TMS application. There must be a <1 °C increase in temperature once TMS has concluded to ensure no damage to brain tissue [3]. See Appendix G for the testing procedure.

## **Electrode Current Generation**

The presence of a secondary induced current must be measured for the duration of TMS testing. Generation of an electric field can be measured using the charge density, which will be less than 30  $\mu$ C/cm² when TMS is being administered at full power [3]. See Appendix H for the testing procedure.

## VII. Discussion

Completion of this phantom will allow Dr. Ahmed and his team to validate the use of TMS in conjunction with iEEG in pediatric patients. A recent study conducted at the University of Iowa tested the use of TMS on adult patients with iEEG [3]. Initial testing was performed

using a gel box phantom, followed by a skull-based phantom to validate the safety of TMS-iEEG. While this phantom addresses several of the current project's concerns, it fails to address more stringent safety standards and physiological differences in applying TMS to pediatric patients with iEEG.

Due to the involvement of pediatric patients, this project requires particular ethical considerations. iEEG is currently approved for use in pediatric patients and is routinely used in surgical planning for patients with uncontrolled seizures. However, TMS is not yet an approved treatment method for use in patients under the age of 15 [59]. While there have been several studies investigating the use of TMS, there is still a lack of formal guidelines for use in pediatric patients. As a research tool, this phantom must accurately represent a pediatric brain in physiological and mechanical aspects in order to collect results on the efficacy of TMS used with iEEG. Responsible conduct of research and development standards must be upheld. A risk analysis should be performed to mitigate potential sources of error. If the final phantom fails in any of the three testing scenarios of electrode displacement, heating, and current generation, the researchers should not proceed with in vivo testing on pediatric patients.

# VIII. Conclusions

Epilepsy is the fourth most common neurological disease, often manifesting in pediatric patients before the age of one year [1]. iEEG is routinely used in surgical planning for epilepsy in adult and pediatric patients. TMS may provide complimentary information for mapping critical regions of the brain that should be avoided during surgery; however, there are still safety concerns around the use of TMS in patients with iEEG electrodes actively implanted. This project aims to develop a phantom for validation of use of TMS in pediatric patients with implanted cortical electrodes. To achieve this, a gel box phantom will be developed for initial testing, followed by a pediatric skull-based phantom. The base of both phantoms will be 3D printed in FBC resin, due to its superior transparency, permittivity, and mechanical properties compared to other options. For the phantom's interior, a brain model will be constructed with an agar hydrogel tuned with NaCl to achieve physiological conductivity. Testing will be performed to determine hydrogel thermal and electrical conductivities and mechanical properties, as well as electrode displacement, heating, and current generation.

# References

- [1] T. A. Milligan, "Epilepsy: A Clinical Overview," *Am. J. Med.*, vol. 134, no. 7, pp. 840–847, July 2021, doi: 10.1016/j.amjmed.2021.01.038.
- [2] G. Askari, M. Vajdi, S. Jafari-Nasab, and S. Golpour-Hamedani, "Ethical guidelines for human research on children and adolescents: A narrative review study," *J. Res. Med. Sci. Off. J. Isfahan Univ. Med. Sci.*, vol. 29, p. 53, Aug. 2024, doi: 10.4103/jrms.jrms\_610\_23.
- [3] J. B. Wang *et al.*, "Effects of transcranial magnetic stimulation on the human brain recorded with intracranial electrocorticography," *Mol. Psychiatry*, vol. 29, no. 5, pp. 1228–1240, May 2024, doi: 10.1038/s41380-024-02405-y.
- [4] C. Minardi *et al.*, "Epilepsy in Children: From Diagnosis to Treatment with Focus on Emergency," *J. Clin. Med.*, vol. 8, no. 1, p. 39, Jan. 2019, doi: 10.3390/jcm8010039.
- [5] F. Winter *et al.*, "Current state of the art of traditional and minimal invasive epilepsy surgery approaches," *Brain Spine*, vol. 4, p. 102755, Jan. 2024, doi: 10.1016/j.bas.2024.102755.
- [6] Y. Wang, J. Yan, J. Wen, T. Yu, and X. Li, "An Intracranial Electroencephalography (iEEG) Brain Function Mapping Tool with an Application to Epilepsy Surgery Evaluation," *Front. Neuroinformatics*, vol. 10, p. 15, Apr. 2016, doi: 10.3389/fninf.2016.00015.
- [7] J.-P. Lefaucheur, "Chapter 37 Transcranial magnetic stimulation," in *Handbook of Clinical Neurology*, vol. 160, K. H. Levin and P. Chauvel, Eds., in Clinical Neurophysiology: Basis and Technical Aspects, vol. 160., Elsevier, 2019, pp. 559–580. doi: 10.1016/B978-0-444-64032-1.00037-0.
- [8] E. N. Sutter, C. P. Casey, and B. T. Gillick, "Single-pulse transcranial magnetic stimulation for assessment of motor development in infants with early brain injury," *Expert Rev. Med. Devices*, vol. 21, no. 3, pp. 179–186, Mar. 2024, doi: 10.1080/17434440.2023.2299310.
- [9] D. Xie, J. Bian, C. Ni, P. Zhao, Z. Pu, and J. Yue, "Tuning Room-Temperature Injectability of Gelatin-Based Hydrogels via Introduction of Competitive Hydrogen Bonds," *ACS Macro Lett.*, vol. 14, no. 3, pp. 313–319, Mar. 2025, doi: 10.1021/acsmacrolett.5c00018.
- [10] F. Mushtaq *et al.*, "Preparation, properties, and applications of gelatin-based hydrogels (GHs) in the environmental, technological, and biomedical sectors," *Int. J. Biol. Macromol.*, vol. 218, pp. 601–633, Oct. 2022, doi: 10.1016/j.ijbiomac.2022.07.168.
- [11] S. P. Pandey, T. Shukla, V. K. Dhote, D. K. Mishra, R. Maheshwari, and R. K. Tekade, "Chapter 4 Use of Polymers in Controlled Release of Active Agents," in *Basic Fundamentals of Drug Delivery*, R. K. Tekade, Ed., in Advances in Pharmaceutical Product Development and Research., Academic Press, 2019, pp. 113–172. doi: 10.1016/B978-0-12-817909-3.00004-2.
- [12] B. Ayyakkalai, J. Nath, H. G. Rao, V. Venkata, S. S. Nori, and S. Suryanarayan, "Chapter 17 Seaweed derived sustainable packaging," in *Applications of Seaweeds in Food and Nutrition*, D. I. Hefft and C. O. Adetunji, Eds., Elsevier, 2024, pp. 263–287. doi: 10.1016/B978-0-323-91803-9.00006-8.
- [13] F. Jiang *et al.*, "Extraction, Modification and Biomedical Application of Agarose Hydrogels: A Review," *Mar. Drugs*, vol. 21, no. 5, p. 299, May 2023, doi: 10.3390/md21050299.
- [14] "3D Printer Dimensions," Google Docs. Accessed: Sept. 25, 2025. [Online]. Available: https://docs.google.com/spreadsheets/d/125EWYr0aojDuu0BGfzzt-YhfGJA1wojkzE-Vt00t w\_M/edit?gid=0&usp=embed\_facebook

- [15] M. Nofar, D. Sacligil, P. J. Carreau, M. R. Kamal, and M.-C. Heuzey, "Poly (lactic acid) blends: Processing, properties and applications," *Int. J. Biol. Macromol.*, vol. 125, pp. 307–360, Mar. 2019, doi: 10.1016/j.ijbiomac.2018.12.002.
- [16] "Polylactic Acid (PLA, Polylactide) :: MakeItFrom.com." Accessed: Oct. 13, 2025. [Online]. Available: https://www.makeitfrom.com/material-properties/Polylactic-Acid-PLA-Polylactide
- [17] "Polymethyl Methacrylate an overview | ScienceDirect Topics." Accessed: Oct. 13, 2025. [Online]. Available: https://www-sciencedirect-com.ezproxy.library.wisc.edu/topics/chemical-engineering/poly methyl-methacrylate
- [18] "BioMed Clear Resin," Formlabs. Accessed: Sept. 25, 2025. [Online]. Available: https://formlabs.com/store/materials/biomed-clear-resin/
- [19] "-ENUS-Clear-Resin-V5-TDS.pdf." Accessed: Sept. 21, 2025. [Online]. Available: https://media.formlabs.com/m/5fd5e7daf1460058/original/-ENUS-Clear-Resin-V5-TDS.pd f
- [20] "Measurement of Ex Vivo Liver, Brain and Pancreas Thermal Properties as Function of Temperature." Accessed: Oct. 13, 2025. [Online]. Available: https://www.mdpi.com/1424-8220/21/12/4236
- [21] A. Antoniou, N. Evripidou, L. Georgiou, A. Chrysanthou, C. Ioannides, and C. Damianou, "Tumor phantom model for MRI-guided focused ultrasound ablation studies," *Med. Phys.*, vol. 50, no. 10, pp. 5956–5968, Oct. 2023, doi: 10.1002/mp.16480.
- [22] X. Xie, D. Li, T.-H. Tsai, J. Liu, P. V. Braun, and D. G. Cahill, "Thermal Conductivity, Heat Capacity, and Elastic Constants of Water-Soluble Polymers and Polymer Blends," *Macromolecules*, vol. 49, no. 3, pp. 972–978, Feb. 2016, doi: 10.1021/acs.macromol.5b02477.
- [23] T. Sakiyama, S. Han, A. Torii, O. Miyawaki, and T. Yano, "Intrinsic Thermal Conductivity of Gelatin Estimated Independently of Heat Conduction Models".
- [24] E. Myers, M. Piazza, M. Owkes, and R. K. June, "Heat conduction simulation of chondrocyte-embedded agarose gels suggests negligible impact of viscoelastic dissipation on temperature change," *J. Biomech.*, vol. 176, p. 112307, Nov. 2024, doi: 10.1016/j.jbiomech.2024.112307.
- [25] A. Sun *et al.*, "Current research progress of photopolymerized hydrogels in tissue engineering," *Chin. Chem. Lett.*, vol. 32, no. 7, pp. 2117–2126, July 2021, doi: 10.1016/j.cclet.2021.01.048.
- [26] G. Satchanska, S. Davidova, and P. D. Petrov, "Natural and Synthetic Polymers for Biomedical and Environmental Applications," *Polymers*, vol. 16, no. 8, p. 1159, Apr. 2024, doi: 10.3390/polym16081159.
- [27] S. Sharifi *et al.*, "Tuning gelatin-based hydrogel towards bioadhesive ocular tissue engineering applications," *Bioact. Mater.*, vol. 6, no. 11, pp. 3947–3961, Nov. 2021, doi: 10.1016/j.bioactmat.2021.03.042.
- [28] "Agar Agar Powder," TM Media. Accessed: Sept. 25, 2025. [Online]. Available: https://www.tmmedia.in/wp-content/uploads/MSDS/MSDS-1201.pdf
- [29] M. Earle, G. D. Portu, and E. DeVos, "Agar ultrasound phantoms for low-cost training without refrigeration.," *Afr. J. Emerg. Med. Rev. Afr. Med. Urgence*, vol. 6, no. 1, pp. 18–23, Mar. 2016, doi: 10.1016/j.afjem.2015.09.003.

- [30] M.-E. Karga, M.-E. Kargaki, H. Iatrou, and C. Tsitsilianis, "pH-Responsive, Thermo-Resistant Poly(Acrylic Acid)-g-Poly(boc-L-Lysine) Hydrogel with Shear-Induced Injectability.," *Gels Basel Switz.*, vol. 8, no. 12, Dec. 2022, doi: 10.3390/gels8120817.
- [31] "Safety Data Sheet (SDS): Poly(acrylic acid)," Chemos. Accessed: Sept. 25, 2025.
  [Online]. Available:
  https://www.chemos.de/import/data/msds/GB\_en/9003-01-4-A0069730-GB-en.pdf
- [32] Z. Zhang, X. Wang, Y. Wang, and J. Hao, "Rapid-Forming and Self-Healing Agarose-Based Hydrogels for Tissue Adhesives and Potential Wound Dressings," *Biomacromolecules*, vol. 19, no. 3, pp. 980–988, Mar. 2018, doi: 10.1021/acs.biomac.7b01764.
- [33] "Safety Data Sheet: Agarose Powder," Fisher Scientific. Accessed: Sept. 25, 2025. [Online]. Available: https://www.fishersci.com/content/dam/fishersci/en\_US/documents/programs/education/reg ulatory-documents/sds/chemicals/chemicals-a/S25128.pdf
- [34] "Safety Data Sheet (SDS)," ATP Type. Accessed: Sept. 25, 2025. [Online]. Available: https://atpgroup.com/wp-content/uploads/2018/06/Gelatin-Rousselot-SDS.pdf
- [35] A. I. Farrer *et al.*, "Characterization and evaluation of tissue-mimicking gelatin phantoms for use with MRgFUS," *J. Ther. Ultrasound*, vol. 3, no. 1, p. 9, June 2015, doi: 10.1186/s40349-015-0030-y.
- [36] S. Mad-Ali, S. Benjakul, T. Prodpran, and S. Maqsood, "Characteristics and gelling properties of gelatin from goat skin as affected by drying methods.," *J. Food Sci. Technol.*, vol. 54, no. 6, pp. 1646–1654, May 2017, doi: 10.1007/s13197-017-2597-5.
- [37] L. Lépine and R. Gilbert, "Thermal degradation of polyacrylic acid in dilute aqueous solution," *Polym. Degrad. Stab.*, vol. 75, no. 2, pp. 337–345, Jan. 2002, doi: 10.1016/S0141-3910(01)00236-1.
- [38] Q.-Q. Ouyang *et al.*, "Thermal degradation of agar: Mechanism and toxicity of products," *Food Chem.*, vol. 264, pp. 277–283, Oct. 2018, doi: 10.1016/j.foodchem.2018.04.098.
- [39] L.-M. Zhang, C.-X. Wu, J.-Y. Huang, X.-H. Peng, P. Chen, and S.-Q. Tang, "Synthesis and characterization of a degradable composite agarose/HA hydrogel," *Carbohydr. Polym.*, vol. 88, no. 4, pp. 1445–1452, May 2012, doi: 10.1016/j.carbpol.2012.02.050.
- [40] "Great Value Unflavored Gelatin Mix, 0.25 oz, 32 Count Pouches," Walmart.com. Accessed: Oct. 13, 2025. [Online]. Available: https://www.walmart.com/ip/Great-Value-Unflavored-Gelatin-Mix-0-25-oz-32-Count-Pouches/531996398
- [41] "Agar powder 500 g | Buy Online | Thermo Scientific Chemicals | thermofisher.com." Accessed: Oct. 12, 2025. [Online]. Available: https://www.thermofisher.com/order/catalog/product/A10752.36
- [42] "Agarose, Electrophoresis Grade 250 g | Buy Online | Thermo Scientific Chemicals | thermofisher.com." Accessed: Oct. 13, 2025. [Online]. Available: https://www.thermofisher.com/order/catalog/product/J66501.30
- [43] "Poly(acrylic acid) average Mv 3,000,000, powder 9003-01-4." Accessed: Oct. 13, 2025. [Online]. Available: https://www.sigmaaldrich.com/US/en/product/aldrich/306223?srsltid=AfmBOoohEpWt90 QcbNACXGLO5NifU4DvKziUsvjTPQ9TChj-B5czavXL
- [44] "Ultimate Guide to PMMA/Acrylic Filament 3D Printing 3DSourced." Accessed: Oct. 13, 2025. [Online]. Available: https://www.3dsourced.com/rigid-ink/pmma-filament-acrylic/

- [45] "Dielectric Properties » IT'IS Foundation." Accessed: Oct. 13, 2025. [Online]. Available: https://itis.swiss/virtual-population/tissue-properties/database/dielectric-properties/
- [46] "Polymethyl Methacrylate (PMMA) Properties." Accessed: Oct. 13, 2025. [Online]. Available: https://matmake.com/materials-data/polymethyl-methacrylate-properties.html
- [47] "(PDF) Analysis of FDM and DLP 3D-Printing Technologies to Prototype Electromagnetic Devices for RFID Applications," *ResearchGate*, Apr. 2025, doi: 10.3390/s21030897.
- [48] L. Falland-Cheung, J. N. Waddell, K. Chun Li, D. Tong, and P. Brunton, "Investigation of the elastic modulus, tensile and flexural strength of five skull simulant materials for impact testing of a forensic skin/skull/brain model," *J. Mech. Behav. Biomed. Mater.*, vol. 68, pp. 303–307, Apr. 2017, doi: 10.1016/j.jmbbm.2017.02.023.
- [49] "3D Printers," Grainger Engineering Design Innovation Lab. Accessed: Sept. 25, 2025. [Online]. Available: https://making.engr.wisc.edu/equipment/3d-printers/
- [50] "Additive Manufacturing | 3D Printing Services," Rapid Prototyping & Low Volume Production. Accessed: Sept. 25, 2025. [Online]. Available: https://www.3erp.com/services/3d-printing/
- [51] "Amazon.com: MSNJ PMMA Filament 1.75mm,PMMA 3D Printer Filament,Dimensional Accuracy +/-0.03 mm,1KG(2.2lb)Spool,Transparent: Industrial & Scientific." Accessed: Sept. 25, 2025. [Online]. Available: https://www.amazon.com/Filament-Printer-Dimensional-Accuracy-Transparent/dp/B08Y5L KNLB
- [52] "-ENUS-Safety-Data-Sheet-BioMed-Clear-Resin.pdf." Accessed: Oct. 12, 2025. [Online]. Available: https://media.formlabs.com/m/1f5f8ab0efaac055/original/-ENUS-Safety-Data-Sheet-BioMed-Clear-Resin.pdf
- [53] "-ENUS-BioMed-Clear-TDS.pdf." Accessed: Sept. 21, 2025. [Online]. Available: https://media.formlabs.com/m/52c8bbc17a4eda5d/original/-ENUS-BioMed-Clear-TDS.pdf
- [54] W. Hou *et al.*, "Design of injectable agar/NaCl/polyacrylamide ionic hydrogels for high performance strain sensors," *Carbohydr. Polym.*, vol. 211, pp. 322–328, May 2019, doi: 10.1016/j.carbpol.2019.01.094.
- [55] A. Hunold, R. Machts, and J. Haueisen, "Head phantoms for bioelectromagnetic applications: a material study.," *Biomed. Eng. Online*, vol. 19, no. 1, p. 87, Nov. 2020, doi: 10.1186/s12938-020-00830-v.
- [56] "What is SLA printing? The original resin 3D print method," Protolabs Network. Accessed: Oct. 12, 2025. [Online]. Available: https://www.hubs.com/knowledge-base/what-is-sla-3d-printing/
- [57] E. Ozkaya *et al.*, "Viscoelasticity of children and adolescent brains through MR elastography," *J. Mech. Behav. Biomed. Mater.*, vol. 115, p. 104229, Mar. 2021, doi: 10.1016/j.jmbbm.2020.104229.
- [58] S. Budday *et al.*, "Mechanical properties of gray and white matter brain tissue by indentation," *J. Mech. Behav. Biomed. Mater.*, vol. 46, pp. 318–330, June 2015, doi: 10.1016/j.jmbbm.2015.02.024.
- [59] C. H. Allen, B. M. Kluger, and I. Buard, "Safety of Transcranial Magnetic Stimulation in Children: A Systematic Review of the Literature," *Pediatr. Neurol.*, vol. 68, pp. 3–17, Mar. 2017, doi: 10.1016/j.pediatrneurol.2016.12.009.

# **Appendix**

# A. Product Design Specifications (PDS)

## Function

Intracranial electroencephalography (iEEG) is routinely used in surgical planning for individuals with uncontrolled seizures, such as those with epilepsy. Utilizing electrode systems either connected across the surface of or implanted into the brain, this method provides high spatiotemporal resolution [1]. Transcranial magnetic stimulation (TMS) assesses brain circuit excitability through electromagnetic induction, inducing currents to produce action potentials and painlessly activate brain networks [2]. While this neuromodulation technique may provide complementary information for mapping out critical brain regions that should be avoided during surgery, there are several safety concerns around the use of TMS in patients with iEEG: that of secondary electrical currents, heating of the implanted electrodes, and electrode array displacement, all of which would have severe consequences for the affected individuals [1]. Additionally, the impact of these techniques has not been previously studied on children with epilepsy, but instead on adult patients: dissimilar physiology and comparative higher resting motor thresholds might require higher levels of stimulation, both of which indicate the need for adjusted treatment [3]. The goal of this project, therefore, is to develop a pediatric brain phantom model that can be used to simulate the main effects of TMS on iEEG electrodes: currents, temperatures, and changes in position.

# **Client requirements**

- 1. The phantom should represent the physiology of the pediatric brain in terms of overall matter volume, approximately 1300 mm<sup>3</sup>, and circumference of the surrounding skull, between 50 to 54 cm [4], [5].
- 2. The material should have efficient conductivity to allow for proper current testing; to represent brain tissue conductivity, this value should lie between 0.2 and 0.5 S/m [6].
- 3. The device must be able to withstand a minimum of 50 magnetic pulses, as is common in TMS sessions for human participants [1].
- 4. The phantom must not physically interfere with TMS coil application to allow for adequate testing. To allow for optimal orientation, the TMS operator should be able to hold the coil within  $5.5 \pm 1.6$  mm of the scalp [7].
- 5. The budget must not exceed \$500.

# **Design requirements**

## 1. Physical and Operational Characteristics

# a. Performance requirements

- i. The phantom must withstand magnetic pulses up to a frequency of 0.5 Hz, as performed in a previous TMS study on patients with implanted electrodes [1].
- ii. To reflect the higher motor threshold present in a pediatric nervous system, as the corticospinal tract continues to develop, the phantom should tolerate pulses up to 2T in magnitude [8], [9].
- iii. Similar physiological properties to the young child brain are ideal, including an overall brain matter volume between 50 and 100 mm<sup>3</sup> and appropriate conductivity levels in the range of 0.2 to 0.5 S/m [4], [5].
- iv. The shape and structure of the model must be maintained despite implantation of electrode arrays up to 90 mm [1].
- v. The construction of the phantom and any necessary container must allow for measurements of displacement, temperature change, and induced current; as such, the device should be accessible from several points, such as from each of the embedded electrodes.

## b. Accuracy and Reliability

- i. After treatment with TMS, the implanted electrodes should experience <1°C of heating [10].
- ii. The iEEG electrodes should experience displacement of less than 20 mm, as some deformations of the brain can naturally occur [11]. Ideally, there will be no significant displacement.
- iii. Charge density must be less than 30  $\mu$ C/cm<sup>2</sup> when TMS is being administered at full power [1].

## c. Life in Service

- i. The phantom will be used to ensure the safety of TMS being used with iEEG technology.
- ii. The phantom must be constructed from material that will not degrade over the entire testing period, such as a 3D printed acrylic polymer. The client will define the length of time in vitro testing with the phantom will occur.
- iii. Each round of TMS testing will last approximately 350 seconds [12].

## d. Shelf Life

- i. The shelf life necessary for this phantom will extend for the duration of client testing. After in vitro testing is complete, the client will begin clinical trials with pediatric patients.
- ii. To ensure minimal material degradation, the phantom will be stored at room temperature and humidity, 22-24 °C and 40-60%, respectively [13].
- iii. Depth electrodes will be used. They will not be permanently implanted but should be used within approximately 3 years [14].

## e. Operating Environment

- i. The phantom will be used in conjunction with TMS and iEEG technology. Materials must be compatible with this technology.
- ii. The phantom will be used in a sterile environment and handled by neurosurgeons during testing.
- iii. The phantom will be used at average room temperature, 22-24 °C, and humidity, 40-60% [13].

## f. Ergonomics

- i. Neurosurgeons handling the phantom must be able to safely use and replace components of the phantom, such as the gel and electrodes, between testing.
- ii. The phantom will be placed on a table for the duration of testing, approximately 1 meter (m) off the ground.

## g. Size

- i. The phantom should mimic the size of an average pediatric brain and skull.
- ii. The approximate volume of the phantom will be 50-100 mm<sup>3</sup> [4].
- iii. The approximate circumference of the skull of the phantom will be 50-54 cm [5].

# h. Weight

i. The phantom will ideally be less than 2 kg to ensure the phantom is easy to transport and lift without causing strain to the user.

#### i. Materials

- i. The base of the phantom will be constructed from a 3D printed acrylic polymer. Acrylic based filament or resin for 3D printing has good optical clarity for viewing access into the phantom and good durability. 3D printed polymethyl methacrylate (PMMA) parts showed minimal degradation over 5 years [15].
- ii. 6-12 contact EEG electrodes will be embedded in silicone for precise positioning of the implanted electrodes [1]. Depth arrays (platinum macro contacts) are implanted while grid arrays (platinum-iridium) are placed on the cortical surface [12].
- iii. A hydrogel will be used to approximate brain tissue. Similar phantoms have used a polyacrylic acid saline gel [1], agar, gelatin, or agarose. The addition of NaCl is necessary to achieve physiologically accurate electrical conductivity [16].
- iv. Fiberoptic fluorescent temperature sensors can be connected perpendicular to the electrodes to measure changes in temperature [12].
- v. Ferromagnetic materials will be avoided so as to not interfere with the TMS induced magnetic field [17].

# j. Aesthetics, Appearance, and Finish

i. The base of the phantom should be 3D printed from a clear filament/resin so that the implanted electrodes and internal components can be easily viewed.

- ii. A replaceable hydrogel brain mimics the texture and conductive properties of the brain. However, a gel with greater optical clarity is desired for positioning and viewing the electrodes.
- iii. A gel-based phantom housed in a rectangular box is better for calibration testing and can be used to evaluate temperature changes and basic electromagnetic effects of TMS [18].
- iv. A skull-based phantom would provide greater anatomical accuracy and more complex geometry is important to evaluate TMS induced fields more realistically [19]. Therefore a combination approach will be taken, where a simpler gel-box phantom will be created for initial testing, before moving onto a more complex skull-based phantom.

## 2. Production Characteristics

## a. Quantity

i. The client desires one gel based phantom housed in a 3D printed rectangular box to first be created for preliminary testing before progressing to a skull-based phantom for improved accuracy.

# b. Target Product Cost

i. The total production cost must not exceed the budget of \$500.

#### 3. Miscellaneous

## a. Standards and Specifications

- i. MTR Standards 2.4 and 3.3 require pediatric patients with implanted electrodes to have an inter-electrode impedance of up 10 kOhms maximum, and that electroencephelograms be run with a reduced sensitivity of 7 microvolts (uV), respectively [20].
- ii. CFR Standard 882.5802 defines the use of TMS coils for treatment of neurological and psychiatric disorders as Class II medical devices with specific controls. Therefore, the testing procedure defined must consider magnetic pulse output, magnetic and electrical field, built in device safety features, and patient exposure to sound during device use [21].
- iii. The testing of the phantom must follow ASTM standard F2182, which details a test procedure for measuring temperature change due to induced current during magnetic resonance applied to implanted devices [22].

## b. Customer

i. The customers for this project are pediatric patients with intracranial implanted electrodes who will need to undergo neurosurgery.

#### c. Patient-related concerns

i. Patient-related concerns during simultaneous iEEG and TMS include heating of electrodes, induced electrical current, and displacement of electrodes. This phantom will investigate the likelihood and severity of each of these concerns on a pediatric patient.

## d. Competition

i. A similar phantom used to test the safety of combined iEEG and TMS was recently made at the University of Iowa [1]. This phantom used a polyacrylic acid (PAA) gel base with a polymethyl methacrylate (PMMA) wall, representing the brain and skull tissue, respectively. This phantom was successfully used to verify safety of concurrent iEEG and TMS use in adult patients undergoing treatment for neuropsychiatric disorders. While this phantom addresses many of the current project's concerns, it fails to account for more stringent safety standards and physiological differences required when considering pediatric patients.

#### **PDS References**

- [1] J. B. Wang *et al.*, "Effects of transcranial magnetic stimulation on the human brain recorded with intracranial electrocorticography," *Mol. Psychiatry*, vol. 29, no. 5, pp. 1228–1240, May 2024, doi: 10.1038/s41380-024-02405-y.
- [2] J.-P. Lefaucheur, "Chapter 37 Transcranial magnetic stimulation," in *Handbook of Clinical Neurology*, vol. 160, K. H. Levin and P. Chauvel, Eds., in Clinical Neurophysiology: Basis and Technical Aspects, vol. 160., Elsevier, 2019, pp. 559–580. doi: 10.1016/B978-0-444-64032-1.00037-0.
- [3] E. N. Sutter, C. P. Casey, and B. T. Gillick, "Single-pulse transcranial magnetic stimulation for assessment of motor development in infants with early brain injury," *Expert Rev. Med. Devices*, vol. 21, no. 3, pp. 179–186, Mar. 2024, doi: 10.1080/17434440.2023.2299310.
- [4] R. a. I. Bethlehem *et al.*, "Brain charts for the human lifespan," *Nature*, vol. 604, no. 7906, pp. 525–533, Apr. 2022, doi: 10.1038/s41586-022-04554-y.
- [5] "Head circumference for age." Accessed: Sept. 13, 2025. [Online]. Available: https://www.who.int/tools/child-growth-standards/standards/head-circumference-for-age
- [6] G. Halnes, T. V. Ness, S. Næss, E. Hagen, K. H. Pettersen, and G. T. Einevoll, *Electric Brain Signals: Foundations and Applications of Biophysical Modeling*, 1st ed. Cambridge University Press, 2024. doi: 10.1017/9781009039826.
- [7] J. Gomez-Tames, A. Hamasaka, I. Laakso, A. Hirata, and Y. Ugawa, "Atlas of optimal coil orientation and position for TMS: A computational study," *Brain Stimulat.*, vol. 11, no. 4, pp. 839–848, July 2018, doi: 10.1016/j.brs.2018.04.011.

- [8] M. Q. Hameed *et al.*, "Transcranial Magnetic and Direct Current Stimulation in Children," *Curr. Neurol. Neurosci. Rep.*, vol. 17, no. 2, p. 11, Feb. 2017, doi: 10.1007/s11910-017-0719-0.
- [9] "TMS (Transcranial Magnetic Stimulation): What It Is," Cleveland Clinic. Accessed: Sept. 14, 2025. [Online]. Available: https://my.clevelandclinic.org/health/treatments/17827-transcranial-magnetic-stimulation-tms
- [10] Y. Fujita *et al.*, "Evaluating the Safety of Simultaneous Intracranial Electroencephalography and Functional Magnetic Resonance Imaging Acquisition Using a 3 Tesla Magnetic Resonance Imaging Scanner," *Front. Neurosci.*, vol. Volume 16, June 2022, doi: 10.3389/fnins.2022.921922.
- [11] A. O. Blenkmann *et al.*, "Anatomical registration of intracranial electrodes. Robust model-based localization and deformable smooth brain-shift compensation methods.," May 11, 2023, *United States*. doi: 10.1101/2023.05.08.539503.
- [12] J. B. Wang *et al.*, "Supplementary information to 'Effects of transcranial magnetic stimulation on the human brain recorded with intracranial electrocorticography." 2024. [Online]. Available: https://static-content.springer.com/esm/art%3A10.1038%2Fs41380-024-02405-y/M ediaObjects/41380\_2024\_2405\_MOESM1\_ESM.pdf
- [13] "Humidity for Hospital and Healthcare Facilities." Accessed: Sept. 14, 2025. [Online]. Available: https://www.neptronic.com/humidifiers/pdf/flyers/Flyer\_Humidity%20for%20Hospitals%20&%20Healthcare EN 20220527.pdf
- [14] "DEN-12SAF: EEG Needles, 12mm x 29 gauge, 48"," Electrode Store. Accessed: Sept. 17, 2025. [Online]. Available: https://electrodestore.com/products/den-12-needles?variant=18289707155518&country=US&currency=USD&utm\_medium=product\_sync&utm\_source=google&utm\_content=sag\_organic&utm\_campaign=sag\_organic&srsltid=AfmBOoojIjxe9i01ONswFljvcAeHpmp2qTiUnwBij6mg3NrGei-Y5iDcwEA
- [15] J. C. Raffaini *et al.*, "Effect of artificial aging on mechanical and physical properties of CAD-CAM PMMA resins for occlusal splints," *J. Adv. Prosthodont.*, vol. 15, no. 5, pp. 227–237, Oct. 2023, doi: 10.4047/jap.2023.15.5.227.
- [16] M. A. Kandadai, J. L. Raymond, and G. J. Shaw, "Comparison of electrical conductivities of various brain phantom gels: Developing a 'Brain Gel Model," *Mater. Sci. Eng. C Mater. Biol. Appl.*, vol. 32, no. 8, pp. 2664–2667, Dec. 2012, doi: 10.1016/j.msec.2012.07.024.
- [17] S. Rossi *et al.*, "Safety and recommendations for TMS use in healthy subjects and patient populations, with updates on training, ethical and regulatory issues: Expert Guidelines," *Clin. Neurophysiol. Off. J. Int. Fed. Clin. Neurophysiol.*, vol. 132, no. 1, pp. 269–306, Jan. 2021, doi: 10.1016/j.clinph.2020.10.003.

- [18] A. Antoniou *et al.*, "MR relaxation times of agar-based tissue-mimicking phantoms," *J. Appl. Clin. Med. Phys.*, vol. 23, no. 5, p. e13533, 2022, doi: 10.1002/acm2.13533.
- [19] H. Magsood and R. L. Hadimani, "Development of anatomically accurate brain phantom for experimental validation of stimulation strengths during TMS," *Mater. Sci. Eng. C*, vol. 120, p. 111705, Jan. 2021, doi: 10.1016/j.msec.2020.111705.
- [20] T. N. Tsuchida *et al.*, "American Clinical Neurophysiology Society Standardized EEG Terminology and Categorization for the Description of Continuous EEG Monitoring in Neonates: Report of the American Clinical Neurophysiology Society Critical Care Monitoring Committee," *J. Clin. Neurophysiol.*, vol. 30, no. 2, p. 161, Apr. 2013, doi: 10.1097/WNP.0b013e3182872b24.
- [21] "eCFR :: 21 CFR 882.5802 -- Transcranial magnetic stimulation system for neurological and psychiatric disorders and conditions." Accessed: Sept. 17, 2025. [Online]. Available: https://www.ecfr.gov/current/title-21/chapter-I/subchapter-H/part-882/subpart-F/sect ion-882.5802
- [22] Standard Test Method for Measurement of Radio Frequency Induced Heating On or Near Passive Implants During Magnetic Resonance Imaging, F2182-19e2.

## **B.** Materials and Expenses

**Table 3. BPAG Expense Sheet** 

Item	Description	Manufac- turer	Mft Pt#	Vendor	Vendor Cat#	Date	#	Cost Each	Total	Link
3D prints										
Formlabs BioMed Clear Sample Swatch	Step wedge with thicknesses of 0.1, 0.2, and 0.3 inches for prelim presentation prop	UW Design and Innovation Lab	N/A	N/A	N/A	10/1	1	\$7.14	\$7.14	
									\$0.00	
Category 2										
									\$0.00	

					\$0.00	
				TOTA	\$7.14	
				L:	Ψ,•11.	

## C. Minitab for Initial Agar and Saline Ratios

- 1. In Minitab go to Stat  $\rightarrow$  DOE  $\rightarrow$  Factorial  $\rightarrow$  Create Factorial Design.
- 2. Choose "General Full Factorial Design" with 2 factors, 3 levels each.
- 3. Click factors and enter:
  - i. Factor A: Agar % (Levels: 2.0, 4.0, 6.0)
  - ii. Factor B: Saline % (Levels: 1.0, 3.0, 5.0)
- 4. Under "Options" select Randomize Runs, Number of Replicates = 3. Click OK to generate the design. This will generate 9 sample combinations with three replicates of each for a total of 27 experiments.
- 5. Fabricate gels using provided sample combinations. Test conductivity of 3 replicates of each.
- 6. Fill in conductivity values collected from the experiment.
- 7. Go to Stat → DOE → Factorial → Analyze Factorial Design. Select the response variable (conductivity).
- 8. View Pareto chart of effects, ANOVA table, and residual plots to determine ideal sample combination.

# D. Use of Rheometer with Hydrogel Testing Protocol

- 1. Turn on the valve to the air line. Do not switch on the rheometer without turning on the air, as it will trip the machine and trigger an emergency shutdown of the system.
- 2. Open the rSpace software on the computer attached to the rheometer.
- 3. Turn on Kinexus Ultra+ Rheometer by using the switch at the back of the machine. Insert cone or plate geometry and allow rheometer to execute its initialization processes. These steps are pre-programmed and automatic

Note: The internal level sensor of this rheometer is not working well recently, and you may find an error message that the machine is not properly labelled. Ignore this message as long as you physically verified the alignment of the rheometer with a spirit level as described in Part II.

- 4. Perform a 2-minute torque map in air. To do this, go to rFinder and search for "Calibration\_0105 Kinexus Torque Mapping.rseq". This step is necessary to calibrate the system before each use of the rheometer.
- 5. Go to rFinder and search for the sequence "General torque sequence.rseq". Select

- to use temperature control, and set the temperature to the desired polymerization temperature in °C. As soon as you see the temperature start to change, you can close the sequence. The rheometer will continue to work towards equilibrium at the polymerization temperature even though you closed the sequence.
- 6. Go to rFinder and search for the sequence "Set Gap.rseq" (there is also a shortcut button for this sequence). Set the gap to 70 mm.
- 7. Go to rFinder and search for the sequence "Set rotational position.rseq". Set the rheometer's absolute position to 3.142 radians. If the upper geometry later gets bumped, or you have other reason to believe the geometry's absolute position is no longer 3.142 radians, repeat this step.
- 8. Use "General torque sequence.rseq" to perform shear testing of the sample. This sequence twists your sample back and forth between two specified absolute positions (which is just the rheometer's term for angular positions) eight times, then returns it to the nominal equilibrium absolute position of 3.142 radians.
- 9. You can select to use temperature control, but if the rheometer is already set to the desired temperature, clicking "no" will simply tell the rheometer to maintain its current temperature. If you click "yes", you can avoid waiting for equilibrium by clicking the "skip" button (the rheometer's definition of thermal equilibrium is quite strict, and can take upwards of 5 minutes to achieve).
- 10. Enter the minimum and maximum angles (absolute positions) that you would like the geometry to twist your sample to.
- 11. Enter the maximum angular velocity you would like rotations to happen at. I recommend .0000351 rad/s. This value ensures quasi-static loading.
- 12. Enter the maximum angular acceleration you would like rotations to happen at. I recommend .0000117 rad/s<sup>2</sup>. This value removes the inertial effect.
- 13. Display the torque vs angle data in rSpace as a table format, and copy them to an excel sheet.
- 14. Then use a MATLAB script to get the best fit modulus from the torque vs angle data.
- 15. Close the rSpace software.
- 16. Switch off the rheometer (switch is at the back of the machine).
- 17. Turn off the air line by closing the valve. This is done for the overall safety of the system and the surroundings when the rheometer is not in use.

# E. Hydrogel Thermal Conductivity Testing Protocol

- 1. Place prepared hydrogel in the phantom skull base.
- 2. Power TLS device on.
- 3. Ensure thermal conductivity probe is properly attached to the device.
- 4. Calibrate device.

- 5. After the device has finished powering on, insert the testing probe until fully submerged, approximately 5 cm.
- 6. Select the testing procedure within the device to measure thermal conductivity.
- 7. Once testing has concluded, remove the probe from the hydrogel and sanitize with ethanol.

## F. Electrode Displacement Testing Protocol

- 1. 10-contact platinum depth electrodes will be implanted into the phantom with 1 cm spacing.
- 2. Place external electrodes on the phantom skull.
- 3. Prepare for TMS by properly calibrating the phantom with the TMS computer program.
- 4. Once calibration has successfully occurred, place the phantom on a stable surface.
- 5. Prepare the high-speed camera to measure at approximately 6664 frames per second (FPS) and begin recording.
- 6. Place the TMS probe on the skull exterior of the phantom, and administer treatment at 100% power.
- 7. End video recording and inspect data.
- 8. Once data is approved, remove the TMS electrodes.
- 9. Analyze video data to determine if any displacement occurred.

## **G.** Electrode Heating Testing Protocol

- 1. 10-contact platinum depth electrodes will be implanted into the phantom with 1 cm spacing.
- 2. Place external electrodes on the phantom skull.
- 3. Prepare for TMS by properly calibrating the phantom with the TMS computer program.
- 4. Once calibration has successfully occurred, place the phantom on a stable surface.
- 5. Place temperature sensors directly on the inserted electrodes.
- 6. Deliver TMS treatment at 100% machine output while taking temperature measurements.
- 7. Detach TMS electrodes from skull base phantom.
- 8. Analyze temperature data and determine degree of heat transfer.

## H. Electrode Current Generation Testing Protocol

- 1. 10-contact platinum depth electrodes will be implanted into the phantom with 1 cm spacing.
- 2. Place external electrodes on the phantom skull.

- 3. Prepare for TMS by properly calibrating the phantom with the TMS computer program.
- 4. Once calibration has successfully occurred, place the phantom on a stable surface.
- 5. Attach oscilloscope probes to two electrodes in parallel and begin measuring peak-to-peak voltage on oscilloscope.
- 6. Administer TMS treatment to the phantom while continuing to measure voltage levels.
- 7. Switch probes to perpendicular orientation, and continue collecting data.
- 8. Once sufficient data has been collected, disconnect the probes from the electrodes.
- 9. Detach TMS electrodes from skull base phantom.
- 10. Analyze data collected from the oscilloscope to determine induced current levels.